Behaviour of Stiffened Steel Plates Subjected to Accidental Loadings

E. Ufuah, *Member, IAENG* and T. H. Tashok

***Abstract*—The behaviour of stiffened steel-plated structures under accidental loadings has not been fully documented. Many research projects that have studied the performance of steel plates have mainly concentrated on those at room temperature design with little information available for fire design. In order to study the behaviour of plates under accidental loading conditions, benchmark structural models were taken from the literature and analysed. This was performed to verify the modelling capability of the numerical tool - ABAQUS in calculating the response parameters at both the heating and cooling phases of a fire. It is recognized that the buckling associated with steel plates are typically resisted by incorporating stiffeners. However, most designers have attempted to utilise the extensional rigidity of plate when the loads are applied in the direction parallel to its plane. Under accidental loading conditions the behaviour can be very different. The findings in this paper demonstrates that under accidental fire loadings, an initial blast can alter the performance of steel plates. For spreading fires, We suggest that the path travelled by the fire can play a significant role in the way the plate will behave under accidental loadings. Moreover, it is noted that the repeated buckling of the plate caused by the travelling fire induces alternating tension and compression in the deck, which is likely to have a major implication on the integrity of welded connections.**

***Index Terms*—Accidental loading, elevated temperature, fire path, stiffened steel plate**

I. Introduction

The behaviour of plated structures under various forms of mechanical loadings has been extensively investigated [1]-[8]. Current research projects have also considered different accidental loadings to which these structures may be subjected [9], [10]. However, the probability of occurrence of accidental loadings such as fire or blast in structures can be very low. In some cases, once a fire has occurred it is often difficult to predict its behaviour and the material performance under this condition becomes more nonlinear. This paper considers the effect of an initial explosion on a plated deck subjected to running pool fires. The numerical tool-ABAQUS [11], implemented to calculate the response parameters, was validated using published data from the literature.

Manuscript received March 23, 2013.

E. Ufuah has just completed his PhD research at the University of Manchester, UK and has been on study leave from Ambrose Alli University, Ekpoma, Nigeria.

(email: ejetrev@yahoo.com)

T. H. Tashok is with Ambrose Alli University, Ekpoma, Nigeria.

(e-mail: yusman_n@yahoo.com).

Under room temperature and fire design, the requirements for steel plated structures do no differ significantly from those for steel framed structures. Primarily, the principal strength members of the former type of structure are plate panels together with support members, whereas the latter comprises truss or beam members whereby the dimension in the axial direction is much greater than those in the other two directions [12]. A thin steel plate is very flexible when it supports loads that act in the direction orthogonal to the plane of the plate. However, it is very rigid when the loads are applied in the direction parallel to its plane. Murray [13] noted that it is this rigidity that engineers attempt to utilise when they design steel-plated structures such as plate girders, box girders, stiffened panels and so on. The main purpose of the stiffeners in this category of structures is to restrain the plates against out-of-plane distortion or buckling. Steel-plated structures will structurally fail when they are loaded beyond their carrying capacity [13], [14]. It should be noted that buckling and yielding of plate members do not occur simultaneously, nevertheless more than one phenomenon will be involved until the structure reaches its ultimate limit state.

For stiffened steel-plated panels, tripping failure of a stiffener, a type of lateral-torsional buckling of the stiffener can be triggered only when a bending effect is applied to induce an initial compression in the flange of the stiffener [15]. Tripping is described in this case as a condition whereby the stiffeners rotate about the line of connection to the plating. However, tripping of a stiffener in a stiffened panel is a function of its torsional capacity. Previous researchers [15]-[18] observed that the torsional stiffness of the stiffener relative to the flexural stiffness of the plate can be a major factor that dictates the failure mode, which may either be plate-induced buckling or stiffener-induced tripping under axial compression.

The concept of stiffened plate in ultimate strength analysis has long provided a means of using plate panels as the basic building elements of many thin-walled steel constructions [13], [19]. A well-known alternative has been the use of folded plates [13], [20]. In most steel-framed structures, there is confidence in relying on the additional strength and stiffness in their post-buckling regime. On the contrary, in slender steel-plated structures with sufficiently high plate slenderness, this is obviously not often the case because once yielding has begun it penetrates quickly through the cross-section as the load increases thus forming local plastic mechanisms [13].

Murray [13] explained that there are circumstances where the behaviour of stiffened plates is difficult to predict. A case with a stiffened panel under in-plane compression

whereby at first the stiffener flange is in tension, then suddenly fails by developing plastic mechanisms in the stiffeners would suggest that the behaviour of the stiffeners may be brittle. Murray [13] further asserted that the failure of one stiffener can instigate failure of the other stiffeners if their behaviour is brittle. Although it is widely known in the literature that post-buckling strength in stiffened plates can be present; yet, their stiffnesses are dramatically reduced at the outset of buckling, perhaps because of the inherent residual stresses resulting from welding. In a fire condition, the strength and stiffness of these structural members are further reduced drastically. The room temperature design of a steel-plated structure is such that as the structure is loaded, the most highly stressed region inside the structural member yields first, thus resulting in local plastic deformation and consequently reducing the member stiffness. As the load increases yet further, the local plastic deformation becomes larger and most likely will occur in several sections within the structural member. This phenomenon induces higher stresses and causes the member stiffness to become quite small thereby culminating in the rapid deflection of the structural member [12], [21].

II. THERMAL AND MECHANICAL PROPERTIES OF STRUCTURAL STEEL

Structural steels of different grades are used in the fabrication of steel work in buildings and other forms structural edifices. There are four categories of steel used for structural application with increasing strengths and stiffnesses ranging from mild carbon steel to heat-treated alloy steel. The behaviour of these groups of steel at room temperature condition is different to that at elevated temperatures. When a steel structure is exposed to fire, the temperature of the element will increase from room temperature to a high level, thereby leaving the material to degrade in strength and stiffness. Eurocode 3 [22] explains that mild carbon steels will begin to degrade in strength once they have attained a temperature of 400^{o}C. Recently, Mäkeläinen et al. [23] and Ufuah [24] have respectively shown that high strength steel and butt-welded connections made with high strength steel grade S420M will begin to degrade in strength only after a temperature value of 100^{o}C is reached.

Moreover, the behaviour of structures at elevated temperatures is typically associated with the period of time at which the structures will survive under exposure to standard fire temperature-time curves before some form of failure begins to manifest. In structural design, strength and stiffness are entirely two important parameters considered together with requirements for ductility, serviceability, weldability, corrosion resistance and so on [12]. The designer, therefore, needs to take cognizance of the changes that occur in the mechanical properties of structural steels.

The thermal properties of carbon and high strength steels at elevated temperatures used in the present investigation are in accordance with Eurocode 3, Part 1.2 [22]. These properties at elevated temperatures, computed using the correlations in Eurocode 3, Part 1.2 [22], are illustrated in Fig. 1. The reduction factors for proportional limit, yield strength and linear elastic range for carbon steel and high strength steel are presented in Figs. 2 and 3 respectively. A representative stress-strain-temperature curve for carbon steel is shown in Fig. 4 whereas the yield values for the various steel sections used in the present study are given in Table 1. The stress-strain model for carbon steel at elevated temperatures is illustrated in Fig. 5. A spreadsheet is usually developed to calculate the stresses and strains in conjunction with the stiffness.

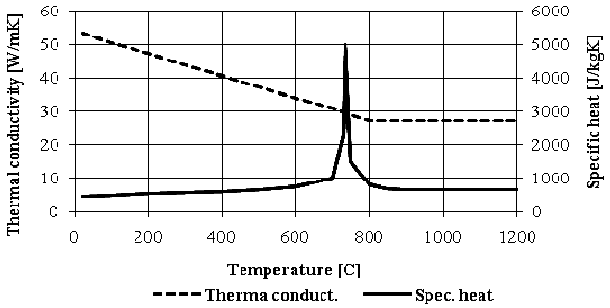

Fig. 1. Thermal properties of carbon steel at elevated temperatures [22]

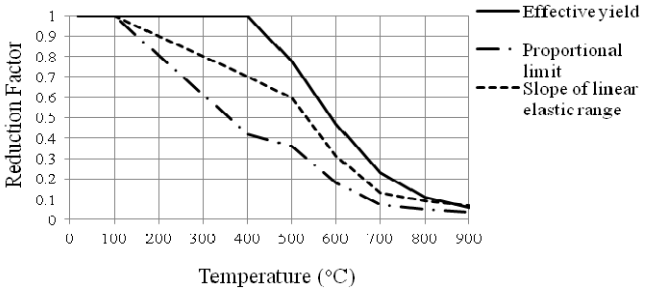

Fig. 2. Reduction factors for yield strength, proportional limit and linear elastic range for high strength steel S420M at elevated temperatures [22].

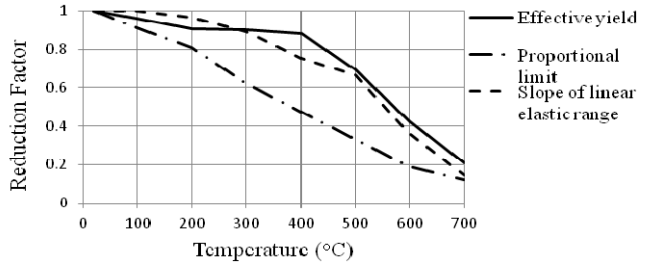

Fig. 3. Reduction factors for yield strength, proportional limit and linear elastic range for high strength steel S420M at elevated temperatures.

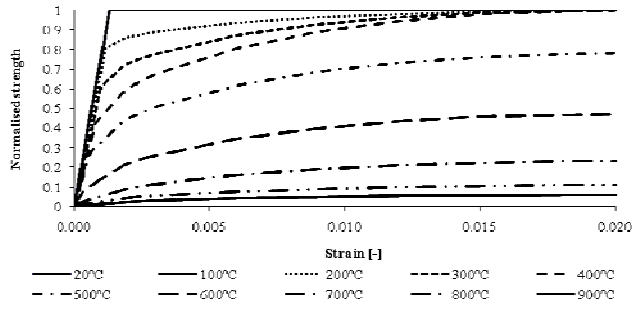

Fig. 4 Stress-strain curves for carbon steel at elevated temperatures [22]

TABLE I
YIELD VALUES FOR STEEL SECTIONS USED IN THE STUDY

Structural Model	Yield Strength (MPa)
Gillie beam model	250
Guedes Soares and Teixeira model	235
Stiffened plate model	420

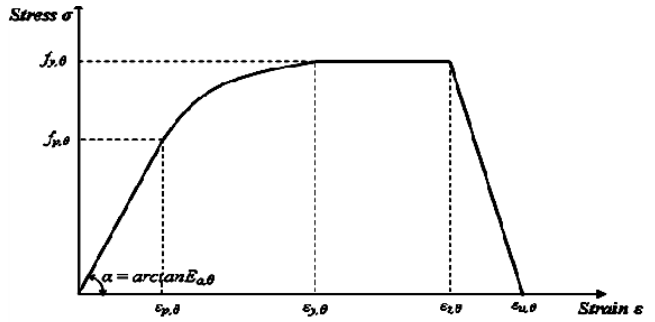

Fig. 5 Stress-strain model for carbon steel at elevated temperatures [22]

III. Modelling Benchmarks

To allow for an accurate prediction of the behaviour of stiffened plate under fire conditions beam and plate models were analysed as benchmark studies, obtained from previous studies [25], [26]. The beam model taken from the study by Gillie [25] has a square profile with dimensions 35mm x 35mm and length 1000mm. The material, geometric and loading conditions are shown in Fig. 6. The geometric and material descriptions of the model were simplified to capture certain behaviours of interest such as the effect of end restraints amongst others in fire conditions. The variable end restraints were determined based on the beam's axial stiffness. To account for the variable end restraints, the support conditions were modelled with spring elements of infinitesimal length located between the beam ends and the reference points along the axis of the beam. Geometric and material nonlinearities were accounted for during the analyses. The slope of linear elastic range was assumed independent of temperature with a magnitude 210 GPa.

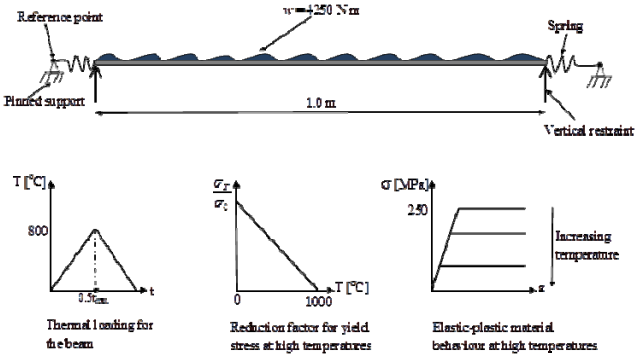

Fig. 6. Loading, geometric and material definitions of the benchmark beam model [25]

The benchmark plate model was taken from the study by Guedes Soares and Teixeira [26]. It consists of a 1000 mm x 1000 mm square plate shown in Fig. 7 with thickness ranging between 16.7 mm and 50 mm. The plate was subjected to a series of localised heating applied to the central portion of the plate in each loading condition. Fire temperature levels were analysed with the heated area ranging from 6 % up to 77 % of the total plate area. An initial distortion of the plate illustrated in Fig. 8 was taken into consideration with the shape of imperfection represented by only the first component of a Fourier series defined by the following correlation:

$$w = \delta \frac{\sin \pi x}{a} \frac{\sin \pi y}{b} \quad (1)$$

where:

a, b represent the two-dimensional spans
δ represents the amplitude

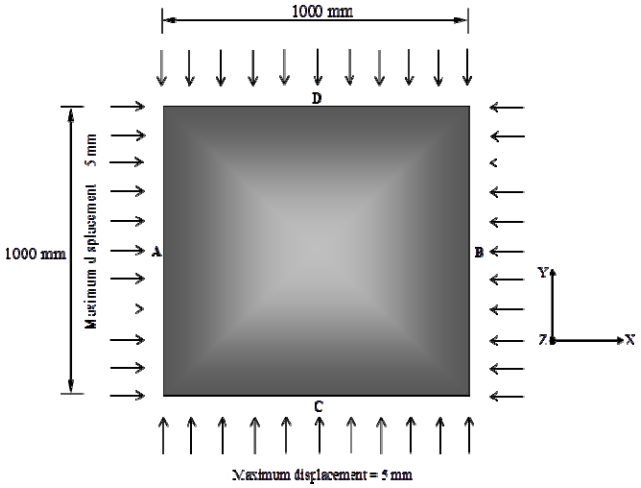

Fig. 7. Imposed displacements for the benchmark plate model

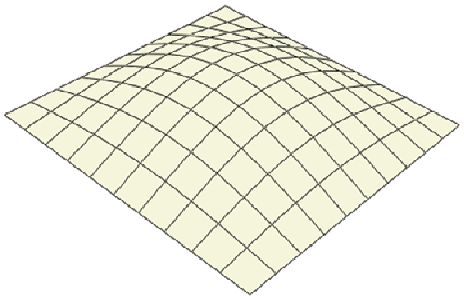

Fig. 8. Shape of initial imperfection for the benchmark plate model

The nominal yield strength and the slope of the linear elastic range for the plate at room temperature are 235 MPa and 200 GPa respectively. The areas subjected to heat load are 25% and 56% of the total plate area with plate slenderness of 20 and 40. The modelling strategy comprises two stages; one that characterises the imperfection while the other introduces the imperfection into the model and executes the structural response. The imperfection was modelled by considering the buckling analysis of the plate using the linear perturbation method to define the initial distorted shape shown in Fig. 8. The amplitude of the imperfection in each of the simply-supported plates was obtained using (2) [26].

$$w_{\max} = 0.15\lambda^2 t \quad (2)$$

where:

$$\lambda = b/t \sqrt{\sigma_o/E}$$

λ is the plate's reduced slenderness, *b* is the plate's width, *t* is the plate's thickness, σ_o is the plate yield and E is the plate's elastic modulus.

The geometry of the series of plate analysed is described

in Table II while the boundary conditions adopted with the corresponding loadings are fully described in Table III. The heat load was applied in a localised area such that the temperatures of 100°C, 200°C, 400°C, 600°C and 800°C were separately considered in the analyses. Once each of these temperature values was attained, an in-plane compression corresponding to an imposed maximum displacement of 5 mm was applied biaxially to simulate the forces induced by restraints to thermal expansion. The strategy adopted here can be explained as follows. As the temperature of the steel plate increases, the plate expands against thermal restraint, which is contributed by the cooler surrounding and the imposed axial loadings thus inducing compression in the plate at the boundaries. These thermal effect and mechanical response occur simultaneously. However, in numerical concept thermal and mechanical fields are sequentially coupled. Therefore, since the heated plate was subjected to biaxial loadings the assumption was to simulate these loadings by imposing a 5 mm axial displacement in each direction.

TABLE II
GEOMETRIC DESCRIPTION OF THE BENCHMARK PLATE MODEL

a (mm)	**b** (mm)	**t** (mm)	**b/t**	**λ**	w_{max} (mm)
1000	1000	50	20	0.686	3.53
1000	1000	25	40	1.371	7.05
1000	1000	16.7	60	2.057	10.6

TABLE III
BOUNDARY AND LOADING CONDITIONS FOR THE BENCHMARK PLATE MODEL

Boundary	**Direction**		**Loading**
	X	Y	
A	$U_x=U_z=U_{Rx}=0$		Thermal loading
B	$U_x=U_z=U_{Rx}=0$		
C		$U_y=U_z=U_{Ry}=0$	
D		$U_y=U_z=U_{Ry}=0$	
A	U_x= 5 mm $U_z=U_{Rx}=0$		Mechanical loading
B	$U_x=U_z=U_{Rx}=0$		
C		U_y= 5 mm $U_z=U_{Ry}=0$	
D		$U_y=U_z=U_{Ry}=0$	

IV. STRUCTURAL MODELLING OF THE STIFFENED PLATE

The stiffened steel-plated structure was initially subjected to an initial explosion and then analysed under fire conditions to ascertain the effect of initial blast on the strength of stiffened plate panel at elevated temperatures. Most offshore structures, according to Liew [27], typically experience explosion before they are further subjected to fire. The stiffened plate shown in Fig. 9 consists of a 2000mm x 2000mm x 25mm square plate securely clamped on all four edges with three equally spaced stiffeners having dimensions 2000mm x 100mm x 12.5mm flat welded to it. Different fire models were employed to study the behaviour of the plate under blast and fire loads. The blast load follows a pressure distribution as given in Table IV. It is likely that an offshore deck will be exposed to an explosion followed by a fire. This may result in an excessive damage to the plated structure. This preliminary investigation, therefore, attempts to assess how plated decks would behaviour under accidental loadings involving both blast and fire. The numerical computations were carried out using a general-purpose commercial code-ABAQUS explicit dynamic [11] analysis in which the plate and stiffeners were modelled using linear S4R-type shell element with finite membrane strains. The numerical tool has the capability of predicting the thermal and mechanical responses of structures based on the finite element method. The large displacement effects of the non-linear finite elements are considered using an updated Lagrangian formulation.

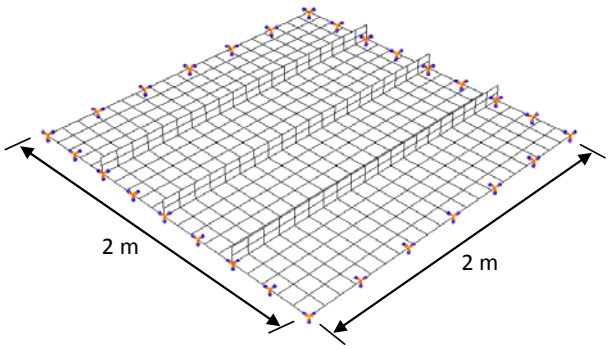

Fig. 9. Stiffened plate subjected to blast and thermal loads

TABLE 1V
BLAST LOAD ON THE STIFFENED PLATE

Time(s)	**Pressure(Pa)**
0.0	0.0
0.001	1000000
0.01	1000000
0.02	0.0
0.05	0.0

The modelling technique includes structural response while incorporating the fire models developed by Ufuah [28] using the power-law methodology and Bailey et al. [29]. The heat loads were directly applied incrementally to the surface nodes of the plate elements using the temperature profiles. The spread of fire follows the fire path depicted in Fig. 10. The arrow represents the direction of travel while the numbers '1' through '4' depicts the different zones. More description can be found in a previous paper by Ufuah [28].

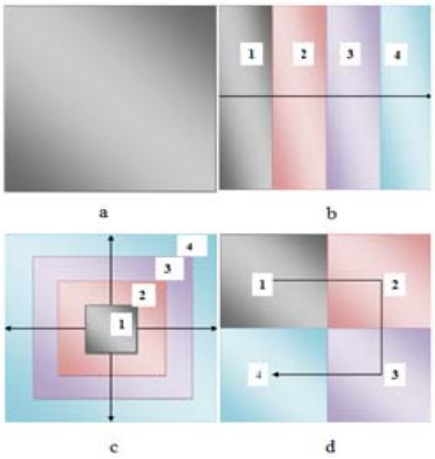

Fig. 10. Fire path used in the study (a) Uniform, (b) Linear and localised, (c) Outward ring and localised, (d) Corner and localised.

However, in sequentially coupled stress analyses, the temperature fields are usually applied to the mechanical

models as forcing functions to calculate the stresses and strains by means of incremental plasticity theory. The multi-linear stress-strain curves at various temperatures describe the non-linear behaviour of the material. The general purpose non-linear finite element analysis code ABAQUS [22] adopts the Newton-Raphson approach to incrementally solve the resulting differential equations. In this condition, the mechanical strength and behaviour of a structural member need to be assessed by employing (3) and (4) [28], [30].

$$\sigma_{ij,j} + f_i = 0 \tag{3}$$

$$\{\Delta\sigma\} = \{D^{ep}\}[B]\{\Delta U_e\} - \{C^{th}\}[M]\{\Delta T_e\} \tag{4}$$

where σ_{ij} is a stress tensor, f_i is a body force, $\Delta\sigma$ is the incremental stress, D^{ep} is the elasto-plastic stiffness, B is strain-displacement relation, U_e is nodal displacement, C^{th} is thermal stiffness, M is temperature shape function and ΔT_e is nodal incremental temperature.

V. RESULTS AND DISCUSSION

In this section the results of the benchmark models and the stiffened plate models are discuss. A comparison of results of the simple benchmark beam model is presented. The calculated mid-span displacement for the beam is shown in Fig. 10. The variation in predictions by the analyses in each case, though negligible, may be drawn from the variation in mesh density, assumptions made in characterising the material model and the size of spring elements assumed. It can be seen that in all cases, but for simple supports condition, an average maximum deflection of 65 mm was achieved when the fire temperature reached 800°C.

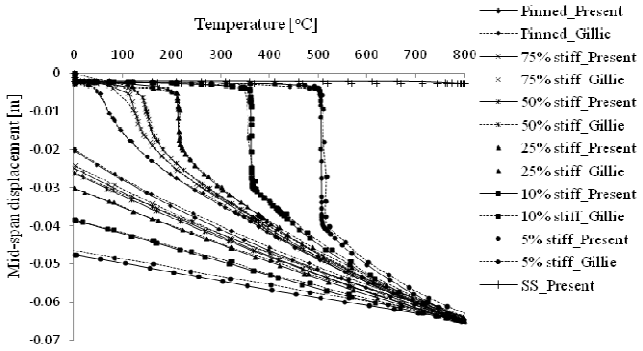

Fig. 10. Comparison of deflection results for the Gillie beam model

The calculated axial stress from the benchmark plate model for the case in which fire is assumed to occupy 56% of the total plate area having a slenderness of 20 (b/t = 20) is shown in Fig. 11. It can be seen that as the fire temperature increases the axial capacity of the plate decreases depending on the slenderness of the plate. The region where the calculated axial stress is situated can be illustrated as an inset in the Fig. 11. The heating of a localised region of the studied plate causes the hot region to expand against thermal restraint produced by the immediate cold surrounding region so that it begins to deflect. At this stage axial compressive forces are induced at the restrained boundaries. As the hot region now begins to cool down and pull on the surrounding the vertical deflection is slightly relieved. The adjacent region then starts to heat up which again causes the plate to deflect further. This further increase in deflection due to a travelling fire is dependent on the form of fire spread as shown in Figs. 12 and 13.

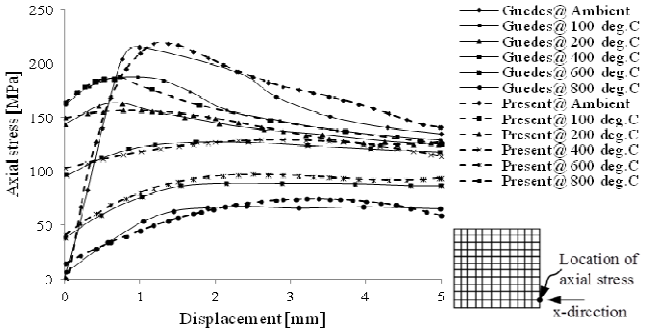

Fig. 11. Axial stress for the case of 56% fire area (b/t = 20)

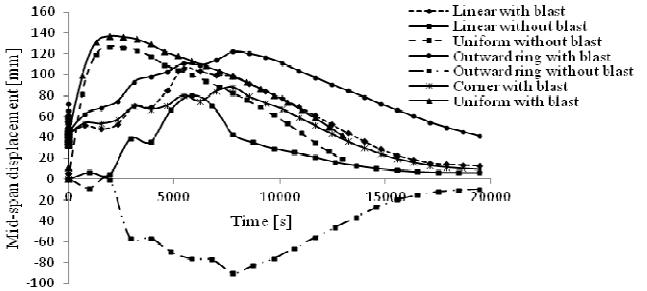

Fig. 12. Mid-span displacement of plate subject to Bailey *et al.* [29] fire load

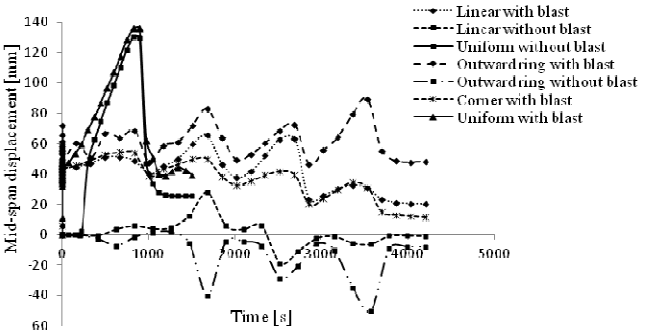

Fig. 13. Mid-span displacement of plate subject to localised fire load

As the fire travels from one zone to the next the localised fire model does not appear to significantly cause any further increase in deflection more than those previously reached as can be seen in Figs. 13. This is probably the case because the fire in the previous zone returns immediately to ambient at the time the fire in the subsequent zone is starting to rise. Two main fire scenarios were studied; one being uniform fire and the other being series of fire spread across four regions on the deck as illustrated in Fig. 10. An investigation into the effect of fire path on structural performance shows that the course of a horizontal fire spread on a stiffened plate can play a significant role on the behaviour of the floor plate. In the case of the plate subjected only to thermal loads, it was assumed that there was no initial displacement prior to the plate being thermally loaded.

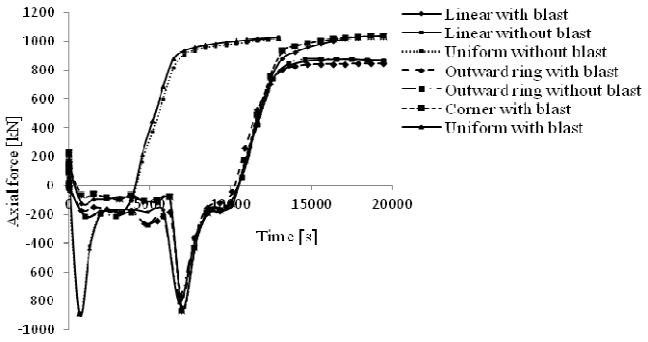

Fig. 14. Axial reactive force in plate subject to Bailey *et al.* **[29]** fire load

The mid-span displacements shown in Figs. 12 and 13 can be further explained by the induced axial forces. The higher the maximum displacement reached under some characteristic loads the lower will be the structural resistance, an explanation which can be demonstrated with the results of the compressive axial capacities of the plate shown in Figs. 14 and 15. In principle, the maximum out-of-plane displacement a structural member can reach is one of the measures for evaluating a plate's capacity under serviceability limit state. As the deck deflects orthogonal to its plane, the carrying capacity weakens as a result of the plastification that may have taken place in some sections within the plate. Therefore, as the mid-span vertical displacement of the plate increases with material degradation its compressive axial capacity reduces correspondingly.

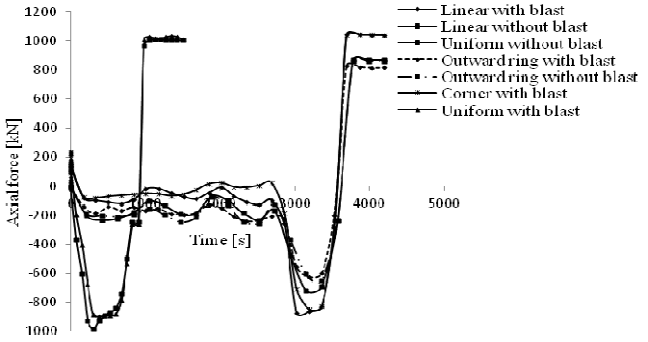

Fig. 15. Axial reactive force in plate subject to localised fire load

REFERENCES

[1] D. D. Milasinovic, "Geometric non-linear analysis of thin plate structures using harmonic coupled finite strip method," Thin-Walled Structures, vol. 49, 2011, pp. 280-290.

[2] M. Boscolo and J. R. Banerjee, "Dynamic stiffness formulation for composite Mindlin plates for exact modal analysis of structures. Part II: Results and applications," Computers and Structures, vol. 96-97, 2012, pp. 74-83.

[3] S. R. Kuo and Y. B. Yang, "A rigid-body-qualified plate theory for the nonlinear analysis of structures involving torsional actions," Engineering Structures, vol. 47, 2013, pp. 2-15.

[4] J. K. Seo, B. J. Kim, H. S. Ryu, Y. C. Ha and J. K. Paik, "Validation of the equivalent plate thickness approach for ultimate strength analysis of stiffened panels with non-uniform thickness," Thin-Walled Structures, vol. 49, 2011, pp. 753-761.

[5] P. Qiao and X Huo, "Explicit local buckling analysis of rotationally-restrained orthotropic plates under uniform shear," Composite Structures, vol. 93, 2011, pp. 2785-2794.

[6] I. Ramu and S. C. Mohanty, "Study of free vibration analysis of rectangular plate structures using finite element method," Procedia Engineering, vol. 38, 2012, pp. 2758-2766.

[7] E. J. Sapountzakis and I. C. Dikaros, "Large deflection analysis of plates stiffened by parallel beams," Engineering Structures, vol. 35, 2012, pp. 254-271.

[8] H. R. Ovesy, S. A. M. Ghannadpour and E. Zia-Dehkordi, "Buckling analysis of moderately thick composite plates and plate structures using an exact finite strip," Composite Structures, vol. 95, 2013, pp. 697-704.

[9] S. E. Quiel and M. E. M. Garlock, "Calculating the buckling strength of steel plates exposed to fire," Thin-Walled Structures, vol. 48, 2010, pp. 684-695.

[10] E. J. Fogle, B. Y. Lattimer, S. Feih, E. Kandare, A. P. Mouritz and S. W. Case, "Compression load failure of aluminium plates due to fire," Engineering Structures, vol. 34, 2012, pp. 155-162.

[11] ABAQUS *Standard/explicit user's manual, Version 6.8-2, vol. 1,2,3 and 4. USA: Dassault Systèmes Simulia Corp*., Providence, RI.

[12] P. K. Paik and A. K. Thayamballi, "Ultimate limit state design of steel-plated structures," John Wiley & Sons, 2002.

[13] N. W. Murray, "Ultimate capacity of stiffened plates in compression," In Narayanan, R. (ed). Plated structures-stability and strength, Applied Science Publishers, 1983, pp. 135-164.

[14] M. R. Khedmati, M. Rastani and K. Ghavami, "Ultimate strength and ductility characteristics of intermittently welded stiffened plates," Journal of Constructional Steel Research vol. 65, 2009, pp. 599-610.

[15] G. Y. Grondin, Q. Chen, A. E. Elwi and J. J. Cheng, "Stiffened steel plates under compression and bending," Journal of Constructional Steel Research vol. 45,(2), 1998, pp. 125–148.

[16] I. A. Sheikh, A. E. Elwi and G. Y. Grondin, "Stiffened steel plates under combined compression and bending," Journal of Constructional Steel Research vol. 59, 2003, pp. 911–930.

[17] I. A. Sheikh, G. Y. Grondin and A. E. Elwi "Stiffened steel plates under uniaxial compression," Journal of Constructional Steel Research vol. 58, 2002, pp. 1061–1080.

[18] G. Y. Grondin, A. E. Elwi and J. J. R. Cheng, "Buckling of stiffened steel plates - a parametric study," Journal of Constructional Steel Research vol. 50, 1999, pp. 151–175.

[19] M. R. Khedmati, M. R. Zareei and P. Rigo, "Empirical formulations for estimation of ultimate strength of continuous stiffened aluminum plates under combined in-plane compression and lateral pressure," Journal of Thin-Walled Structures vol. 48, 2010, pp. 274–289.

[20] S. Haldar and A. H. Sheikh, "Bending analysis of composite folded plates by finite element method," J. Finite Element in Analysis and Design, vol. 47, 2011, pp. 477-485.

[21] R. Szilard, "Theory and analysis of plates: Classical and numerical methods. Prentice-Hall Inc, 1974.

[22] *European Committee for Standardization CEN, Eurocode 3, Design of steel Structures- Part 1-2; BS EN 1993-1-2*, General Rules-Structural Fire Design, 2005.

[23] P. Mäkeläinen, J. Outinen and J. Kesti, "Fire design models for structural steelS420M based upon transient state tensile test results," J Constr. Steel Research, vol. 48, 1998, pp. 47-57.

[24] E. Ufuah, "Characterization of elevated temperature mechanical properties of butt-welded connections made with HS steel grade S420M," J. Lecture Notes in Engineering and Computer Science, vol. 2199(1), 2012, pp. 1755-1760.

[25] M. Gillie, "Analysis of heated structures: nature and modelling benchmarks," Fire Safety Journal, vol. 44, 2009, pp. 673-680.

[26] C. Guedes Soares, and A. P. Teixeira, "Strength of plates subjected to localised heat loads," J Constr. Steel Research, vol. 53, 2000, pp. 335-358.

[27] R. J. Y. Liew, "Survivability of steel frame structures subject to blast and fire," J Constr. Steel Research, vol. 64, 2008, pp. 854-866.

[28] E. Ufuah, "The behaviour of stiffened steel plated decks subjected to unconfined pool fires," Proceedings of the World Congress on Engineering and Computer Science, San Francisco, USA, vol. II, WCECS 2012, October 24-26, 2012.

[29] C. G., Bailey, I. W., Burgess, and R. J., Plank, "Analysis of the effects of cooling and fire spread on steel-framed buildings," Fire Safety Journal, vol. 26, 1996, pp. 273-293.

[30] T-L. Teng, P-H Chang, and W-C Tseng, "Effect of welding sequences on residual stresses", Journal of Computers and Structures, vol. 81, 2003, pp. 273–286.